Poultry Science

Whole genome resequencing reveals genomic regions related to red plumage in ducks

Xinye Zhang,[*] Fangxi Yang,[†] Tao Zhu,[*] Xiurong Zhao,[*] Jinxin Zhang,[*] Junhui Wen,[*] Yalan Zhang,[*] Gang Wang,[*] Xufang Ren,[*] Anqi Chen,[*] Xue Wang,[‡] Liang Wang,[§] Xueze Lv,[§] Weifang Yang,[§] Changqing Qu,[#] Huie Wang,[¶] Zhonghua Ning,[*] and Lujiang Qu [*,1]

[*]*Department of Animal Genetics and Breeding, National Engineering Laboratory for Animal Breeding, College of Animal Science and Technology, China Agricultural University, Beijing 100193, China;* [†]*Beijing Nankou Duck Breeding Technology Co., Ltd., Beijing, China;* [‡]*VVBK Animal Medical Diagnostic Technology (Beijing) Co., Ltd, Daxing District, Beijing, China;* [§]*Beijing Municipal General Station of Animal Science, Beijing, China;* [#]*Engineering Technology Research Center of Anti-aging Chinese Herbal Medicine of Anhui Province, Fuyang Normal University, Fuyang, China; and* [¶]*College of Animal Science, Tarim University, Xinjiang, China*

ABSTRACT Plumage color is a characteristic trait of ducks that originates as a result of natural and artificial selection. As a conspicuous phenotypic feature, it is a breed characteristic. Previous studies have identified some genes associated with the formation of black and white plumage in ducks. However, studies on the genetic basis underlying the red plumage phenotype in ducks are limited. Here, genome-wide association analysis (**GWAS**) and selection signal detection (Fst, $\theta\pi$ ratio, and cross-population composite likelihood ratio [**XP-CLR**]) were conducted to identify candidate regions and genes underlying duck plumage color phenotype. Selection signal detection revealed 29 overlapping genes (including *ENPP1* and *ULK1*) significantly associated with red plumage color in Ji'an Red ducks. *ENSAPLG00000012679, ESRRG,* and *SPATA5* were identified as candidate genes associated with red plumage using GWAS. Selection signal detection revealed that 19 overlapping genes (including *GMDS, PDIA6*, and *ODC1*) significantly correlated with light brown plumage in Brown Tsaiya ducks. GWAS to narrow down the significant regions further revealed nine candidate genes (*AKT1, ATP6V1C2, GMDS, LRP4, MAML3, PDIA6, PLD5, TMEM63B*, and *TSPAN8*). Notably, in Brown Tsaiya ducks, *GMDS, ODC1*, and *PDIA6* exhibit significantly differentiated allele frequencies among other feather-colored ducks, while in Ji'an Red ducks, *ENSAPLG00000012679* has different allele frequency distributions compared with that in other feather-colored ducks. This study offers new insights into the variation and selection of the red plumage phenotype using GWAS and selective signals.

Key words: duck, selection signal detection, genome-wide association analysis, plumage color

2024 Poultry Science 103:103694
https://doi.org/10.1016/j.psj.2024.103694

INTRODUCTION

Bird plumage exists in various colors. In natural environments, plumage color diversity is usually associated with mating signals and camouflage adaptations to different surroundings. Similarly, human preferences for color have influenced poultry plumage coloration during selective breeding. Plumage color is primarily determined by melanin. Variations in color depths result from differences in the relative distribution and abundance of 2 types of melanin, that is, eumelanin (brown/black) and pheomelanin (yellow/red) (Serra, 1946). Melanin is synthesized within melanocytes. Variations in factors involved in the generation, migration, proliferation, and differentiation of melanocytes can impact melanin production, causing changes in plumage color (Yang et al., 2017; Huang et al., 2020; Hua et al., 2021).

Many genes influencing variation in plumage color phenotype have previously been identified. Extension/melanocortin-1 receptor (***MC1R***) is crucial in melanin synthesis, influencing various pigment deposition traits in mammals and bird species, including mice (Robbins et al., 1993), pigs (Kijas et al., 1998), sheep (Vage et al., 1999), chickens (Kerje et al., 2003), and ducks (Yu et al., 2013). The dominant white plumage color trait in

Received January 26, 2024.
Accepted March 25, 2024.

[1]Corresponding author: quluj@163.com

chickens is associated with *PMEL17*, whereas the recessive white plumage color trait is related to *TYR*. In ducks, mutations and large intronic insertions in *MITF* cause the white plumage phenotype (Zhang et al., 2018; Zhou, et al., 2018). The mottled plumage color trait in chickens is caused by the *EDNRB2* mutation (Kinoshita et al., 2014). Similarly, the dark-brown plumage color in chickens is caused by the deletion of a large upstream segment of *SOX10* (Gunnarsson et al., 2011).

According to Chinese Poultry Genetic Resources, the Ji'an Red duck is a local specialty breed from Ji'an, Jiangxi, China, known for its red feathers, medium size, beautiful appearance, adaptability, and high egg production, which is cultivated into excellent raw material for plate duck after scientific and systematic selection and breeding. It has wide application prospects. The Brown Tsaiya duck is from Taiwan, China, and is characterized by its light brown feathers, small body size, and high egg production. However, studies on the genetic basis of red/light brown plumage color phenotypes in ducks are limited. Analyzing the reasons for the formation of their plumage color can provide a rational basis for selecting breeds and marking-assisted selection of Ji'an Rd and Brown Tsaiya ducks. Here, we reported the whole genome sequences of 18 red-feathered ducks, including 10 Brown Tsaiya and 8 Ji'an Red. We conducted a genome-wide association study (**GWAS**) and selection signal detection to identify candidate genes and regions associated with the red plumage color trait in ducks by integrating these data with our previously obtained and 13 publicly available samples. This study contributed to advancing our understanding of the duck plumage color genetics, thereby helping to improve varieties.

MATERIALS AND METHODS

We collected 103 ducks from 12 different breeds. The Brown Tsaiya and Ji'an Red ducks were obtained from the Taiwan and Fujian Provinces (China), respectively. The remaining duck samples were obtained from our previous studies (Zhang et al., 2018; Zhu et al., 2021; Zhang et al., 2023b). We downloaded 13 sets of sequencing data from NCBI. Their detailed information (including breed names, plumage color phenotypes, sampling locations, and primary sequence accession numbers) is presented in Table 1 and Table S1. Blood samples were collected through standard venipuncture. Genomic DNA was extracted using the TIANamp Genomic DNA Kit (TIANGEN Biotech, Beijing, China), according to the manufacturer's instructions. DNA concentration and quality were detected using NanoDrop. For genome sequencing, 2 paired-end libraries with an insert size of 500 bp were constructed and sequenced using the Illumina HiSeq 2500 platform. The average raw read sequence coverage of the duck population is 5x. The animal experimentation protocols were approved by the Animal Welfare Committee of China Agricultural University (permit XK622, Permit 046/2018), and the study was performed following ethical guidelines for animal research.

Alignments and Variant Identification

The raw data were filtered using default parameters using fastp (v0.20.0) (Chen et al., 2018) to avoid low-quality reads. All cleaned reads were aligned to the duck reference genome (cau_duck1.0) using BWA-MEM (v0.7.15) (Li and Durbin, 2009). The Genome Analysis Toolkit (GATK v4.1.8.1) (McKenna et al., 2010) was used for the realignment of reads and SNP calling. The 'SortSam' command of GATK was used to convert the alignment results to the bam format and read sorting by coordinate. We performed quality control on the generated variant set using the default GATK parameters, retaining only high-quality SNP. Single nucleotide polymorphisms were filtered using the following standards: (a) QUAL > 30.0, (b) QualByDepth (QD) > 5.0, (c) FisherStrand (FS) < 60.0, (d) RMS MappingQuality (MQ) > 40.0, (e) MappingQualityRankSunTest (MQRankSum) > -12.5, and (f) ReadPosRankSum > -8.0. Finally, 11,938,694 SNP were retained for the subsequent association analysis.

Population Structure Analysis

Plink (v1.9) (Chang et al., 2015) was used for principal components analysis (**PCA**) to generate eigenvectors and eigenvalues. The first 2 principal components were selected as the x and y coordinates, and the data were visualized using the plot function in R.

Table 1. Summary of individuals used in this study.

Breed	Abbreviation	Sample size	Geographic origin	Phenotype	Sample origin
Ji'an Red duck	JAN	13	This study; Jiang et al., 2021; Zhou et al., 2018	red	Jiangxi, China
Brown Tsaiya duck	HC	10	This study	light brown	Taiwan, China
Wendeng Black duck	WD	8	Zhang et al., 2023b	black	Shandong, China
Putian Black duck	PT	8	Zhang et al., 2023b	black	Fujian, China
Longsheng-Cui duck	LONGS	8	Wang et al., 2021	black	Guangxi, China
Spot-billed duck	BZ	8	Zhu et al., 2021	hemp	Ningxia, China
Mallard	MD	8	Zhang et al., 2018	hemp	Zhejiang, China
Gaoyou duck	GY	8	Zhang et al., 2018	hemp	Jiangsu, China
Jinding duck	JD	8	Zhang et al., 2018	hemp	Fujian, China
Mei duck	MEI	8	Zhu et al., 2021	hemp	Anhui, China
Shanma duck	SM	8	Zhang et al., 2018	hemp	Fujian, China
Shaoxing duck	SX	8	Zhang et al., 2018	hemp	Zhejiang, China

Genome-Wide Selective Sweep Analysis

Selective sweeps between populations with red and other plumage colors were detected using Fst, $\theta\pi$ ratio, and cross-population composite likelihood ratio (**XP-CLR**). The Fst value and $\theta\pi$ ratio were calculated with 10-kb windows and slides with 5-kb steps using VCFtools (v0.1.13) (Danecek et al., 2011). XP-CLR was calculated with 10-kb windows and slides with 5-kb steps. In each approach, windows within the top 1% values were considered significant. Overlapping windows within the top 1% values of Fst, $\theta\pi$ ratio, and XP-CLR were simultaneously regarded as candidate selection regions.

GWAS

A univariate mixed linear model in GEMMA (v0.98.1) (Zhou and Stephens, 2012) was used to identify SNPs significantly associated with plumage color phenotype traits. The models are as follows:

$$y = W\alpha + x\beta + u + \epsilon$$

where y denotes the vector of phenotypic values for individuals, W is the matrix of covariates, α denotes the vector of corresponding coefficients comprising the intercept, x is the vector of marker genotypes, β is an estimate of the marker/SNP additive effect, u is the vector of random effects, and ϵ is the vector of errors. The Manhattan and Quantile-Quantile plots were drawn using the R package "CMplot" package.

Candidate Gene Analysis

We used Ensembl (http://www.ensembl.org/biomart/martview/) for gene annotation. Metascape (https://metascape.org/gp/index.html) was used for the biological function and relevant pathway analyses. Beagle (v5.4) software (Browning et al., 2018) was used to construct haplotypes within the target regions. Additionally, allele frequencies and π statistics were calculated to verify the candidate sweep regions.

RESULTS

Population Structure

PCA showed a distinct stratification between domesticated breeds and wild populations based on the first principal components (PC1). Additionally, a distinct separation was observed between brown mallards and domestic duck populations based on the second principal components (PC2) (Figure 1).

Association Analysis of Red Plumage Phenotype in Ji'an Red Ducks

Selecting Plumage Color Traits To identify the selection signature associated with red plumage, we searched the duck genome for regions using 3 statistical methods (Fst, π ratio, and XP-CLR) to compare the populations of red (JAN) and non-red (MD, BZ, JD, SX, GY, SM, MEI, WD, PT, and LONGS) plumage ducks based on sliding 10-kb windows with 5-kb steps (Figure 2). The regions within the top 1% values were considered candidate genomic regions. We identified 227, 305, and 538 candidate genes through Fst, π-ratio, and XP-CLR, respectively. On combining Fst, π ratio, and XP-CLR analyses, we identified 29 overlapping selected genes, including *DCN, ENPP1, ESRRG, FGD4, GALNT1, GALNTL6, HAPLN1, RASSF6, RIMKLB, SKAP1, SLC25A21, SPAG16, SPATA5, SRGAP1, TPK1*, and *ULK1* (Table 2). In our list of overlapping selected genes, *ENPP1* and *ULK1* were notable owing to their association with pigment deposition.

GWAS for Plumage Color Traits Subsequently, we used the red plumage group as the case and the non-red group as the control and performed GWAS to identify candidate genes that influence the plumage color traits in Ji'an Red ducks (Figure 3). We found 3 significant peaks on chromosomes 3, 10, and 21, with 418 significant SNPs. Ensembl was used to annotate significant SNPs. Fifty-five genes were identified around significant peaks. The most significant SNP (chr10: 15076449; −log10p = 16.88) was in *ENSAPLG00000012679*. *ESRRG* and *SPATA5* overlap within the top 1% windows detected in the selection signal scan of Ji'an Red ducks against other non-red-feathered duck populations, prompting more comprehensive future studies.

Analyzing Candidate Genes The genomic architecture of the candidate genes in different plumage populations was analyzed by calculating the allele frequency. Notably, *ENSAPLG00000012679* exhibited significant differences in allele frequency between Ji'an Red ducks and other plumage populations (Table S2), as verified in the haplotype comparison analysis (Figure 4).

Association Analysis of Red Plumage Phenotype in Brown Tsaiya Ducks

Selecting Plumage Color Traits To identify the selection signature associated with red plumage in Brown Tsaiya ducks, we employed the same methods that were used in Ji'an Red ducks (Figure 5). We identified 253, 371, and 490 candidate genes through Fst, π-ratio, and XP-CLR, respectively. On combining Fst, π ratio, and XP-CLR analyses, we identified 19 overlapping selected genes (*AKT1, ARHGAP15, ATP6V1C2, CCDC149, FNTA, GMDS, ITGB1BP1, LRFN2, LRP4, LY75, MAML3, ODC1, PDIA6, PEX5L, PLD5, RBPJ, SLC4A7, TMEM63B,* and *TSPAN8*) (Table 3). These genes are potentially associated with light brown plumage color in Brown Tsaiya ducks. In our overlapping selected gene list, *GMDS, PDIA6, and ODC1* were notable owing to their association with pigment deposition.

GWAS for Plumage Color Traits GWAS was performed in Brown Tsaiya ducks to further support results

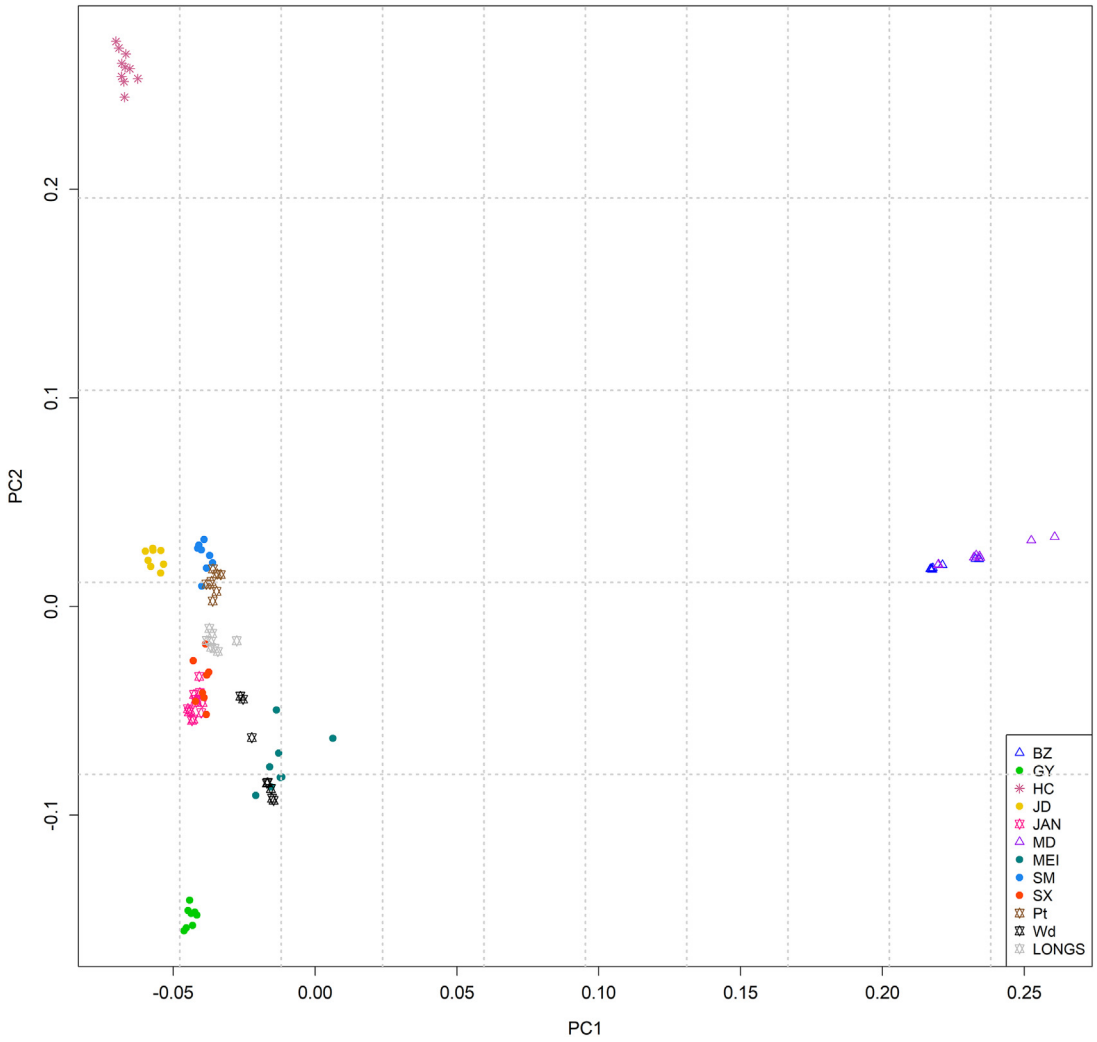

Figure 1. Principal components analysis (**PCA**) plot of duck populations in this study Each color represents a breed, and the abbreviations are as defined in Table 1.

from the selection sweep analysis (Figure 6). There were 3 significant peaks on chromosomes 1, 3, and 11, with 2,224 significant SNPs. Among the significant SNPs, 197 candidate genes were annotated. The most significant SNP (chr11: 1844022; −log10p = 57.32) was in *AP4E1*. Additionally, *AKT1, ATP6V1C2, GMDS, LRP4, MAML3, PDIA6, PLD5, TMEM63B,* and *TSPAN8* were annotated and overlapped within the top 1% windows detected in the selection signal scan of Brown Tsaiya ducks against other non-red-feathered duck populations. Similarly, 2 overlapping genes associated with pigment deposition (*PDIA6* and *GMDS*) were identified using GWAS and selection signal detection and require focus.

Analyzing Candidate Genes We calculated the allele frequency differences between Brown Tsaiya and other duck breeds with respect to these significant genes and observed that *GMDS, ODC1,* and *PDIA6* exhibited significant differences between Brown Tsaiya and other duck breeds (Tables S3, S4, and S5); the same was verified in the haplotype comparison analysis (Figure 7; Figures S1 and S2).

DISCUSSION

During extended domestication and breeding processes, Ji'an Red and Brown Tsaiya ducks exhibit distinct plumage color phenotypes (red/light brown). Ji'an Red and Brown Tsaiya ducks are among the few domestic duck breeds characterized by their red plumage, that holds substantial cultural and economic significance. Therefore, studying candidate genes associated with plumage color traits is essential. Natural and artificial selection significantly influences the genome during animal domestication. Rapidly advancing sequencing technologies provided greater convenience for studying genetic variations associated with phenotypes. In this study, we performed GWAS and selection sweep analysis using SNPs derived from whole genome sequencing on 103 duck samples and identified candidate genes associated with the red plumage phenotype.

In Ji'an Red ducks, we analyzed the genetic basis of the red plumage trait through selection signal analysis and GWAS and identified 19 overlapping genes. Among these genes, *ENPP1* (encoding ectonucleotide

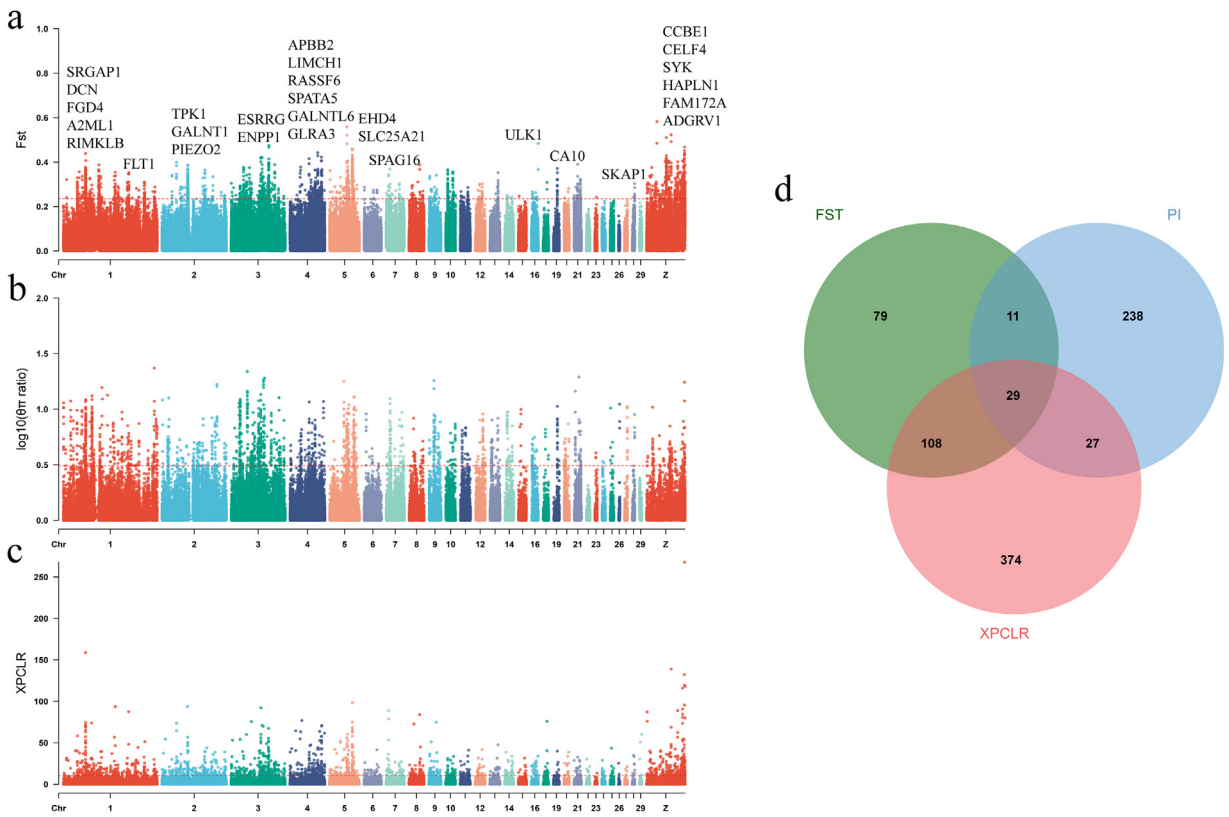

Figure 2. Selective signals of red plumage color in Ji'an Red duck. (A) Genome wide distribution of Fst. (B) Genome wide distribution of $\theta\pi$ ratio. (C) Genome wide distribution of XP-CLR. (D) Fst, $\theta\pi$ ratio, and XP-CLR screened for overlapping genes.

Table 2. Overlapping significant regions identified through Fst, pi, and cross-population composite likelihood ratio (**XP-CLR**) and associated genes in Ji'an red duck.

Gene	Full Name	Chromosome	Location (bp)[1]	Length (bp)[1]	Number (SNP)[2]
FLT1	Fms-related receptor tyrosine kinase 1	1	140607629-140714774	107145	0
SRGAP1	SLIT-ROBO Rho GTPase activating protein 1	1	34632585-34784998	152413	0
DCN	Decorin	1	47576720-47618330	41610	0
FGD4	FYVE, RhoGEF and PH domain containing 4	1	61408749-61520984	112235	0
A2ML1	alpha-2-macroglobulin like 1	1	78744053-78759702	15649	0
RIMKLB	Ribosomal modification protein rimK like family member B	1	78809659-78868404	58745	0
PIEZO2	Piezo-type mechanosensitive ion channel component 2	2	108182771-108436216	253445	0
TPK1	Thiamin pyrophosphokinase 1	2	56610690-56924039	313349	0
GALNT1	Glycine receptor alpha 3	2	88805150-88885411	80261	0
ESRRG	Estrogen-related receptor gamma	3	19239319-19591403	352084	2
ENPP1	Ectonucleotide pyrophosphatase/phosphodiesterase 1	3	59439252-59495836	56584	0
APBB2	Amyloid beta precursor protein binding family B member 2	4	41121623-41293764	172141	0
LIMCH1	LIM and calponin homology domains 1	4	41347255-41516480	169225	0
RASSF6	Ras association domain family member 6	4	46531424-46545165	13741	0
SPATA5	Spermatogenesis associated 5	4	50364115-50553393	189278	2
GALNTL6	Polypeptide N-acetylgalactosaminyltransferase like 6	4	67885840-68340827	454987	0
GLRA3	Glycine receptor alpha 3	4	69037780-69126058	88278	0
EHD4	EH domain containing 4	5	30785990-30809368	23378	0
SLC25A21	Solute carrier family 25 member 21	5	38842670-39100823	258153	0
SPAG16	Sperm-associated antigen 16	7	7830019-8217436	387417	0
ULK1	Unc-51-like autophagy activating kinase 1	16	2432092-2511157	79065	0
CA10	Carbonic anhydrase 10	19	8107861-8307451	199590	0
SKAP1	Src kinase-associated phosphoprotein 1	28	4928465-5045546	117081	0
CCBE1	Collagen and calcium binding EGF domains 1	Z	12928073-13020979	92906	0
CELF4	CUGBP Elav-like family member 4	Z	2270219-2590923	320704	0
SYK	Spleen-associated tyrosine kinase	Z	47469844-47525435	55591	0
HAPLN1	Hyaluronan and proteoglycan link protein 1	Z	75004898-75063923	59025	0
FAM172A	Family with sequence similarity 172 member A	Z	79206564-79452504	245940	0
ADGRV1	Adhesion G protein-coupled receptor V1	Z	80535623-80810901	275278	0

[1]Source: Reference cau_duck1.0 primary assembly (Ensembl).
[2]The number of genomes significant SNP located in gene identified in genome-wide association analysis

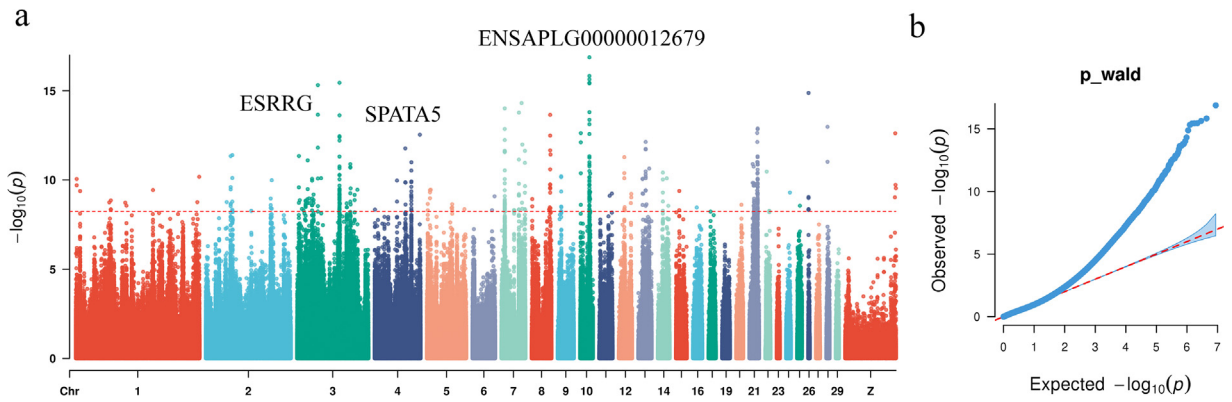

Figure 3. Genome-wide association study for red plumage color in Ji'an Red duck. (A) Manhattan plot of genome-wide association study. (B) Quantile−quantile (Q−Q) plots from the genome-wide association analysis (**GWAS**).

pyrophosphatase/phosphodiesterase 1) and *ULK1* were associated with pigment deposition. The somatomedin-B-like 2 (SMB2) domain of *ENPP1* affects epidermal pigmentation and differentiation (Eytan et al., 2013). A missense mutation in *ENPP1* can reportedly induce the development of hyperpigmented lesions with hypopigmented macules, causing a hereditary skin disorder (Chourabi et al., 2018). *ULK1* regulated melanin levels, where its depletion increased *TYR* and *MITF* transcriptions (Ho et al., 2011; Kalie et al., 2013). In addition to the candidate genes associated with pigmentation, *ENPP1* and *ULK1*, 2 other overlapped genes were detected through GWAS, *ESRRG*, and *SPATA5*. *ESRRG* is involved in steroid hormone-mediated signaling pathway and is essential in the development of the renal papilla (Berry et al., 2011). *SPATA5* correlates with brain development (Buchert et al., 2016; Tanaka et al., 2015). Other candidate genes were related to growth and development, the nervous system, and fat deposition. The mechanism underlying red plumage is unknown in ducks. We speculated that these genes may influence the development of the red plumage phenotype in Ji'an Red ducks; however, their precise mechanisms of action remain unclear.

We performed selection signal detection (including Fst, $\theta\pi$ ratio, and XP-CLR) on Brown Tsaiya ducks and identified 19 overlapped genes with diverse functions, indicating that plumage color is a complex multifactorial trait. Among the candidate genes, those associated with pigment deposition include *GMDS, PDIA6*, and *OCD1*. *GMDS* is associated with pigmentation traits in chickens (Nie et al., 2016) and is related to the non-white wool trait in sheep (Zhang et al., 2023a). *PDIA6* is a member of the protein disulfide isomerase family that activates the Wnt/β-catenin pathway (Gao et al., 2016). The Wnt/β-catenin signaling pathway plays a crucial role in melanogenesis (Liu et al., 2023). *PDIA6* is a candidate gene for pigmentation in East Asian populations (Hider et al., 2013). Increased *ODC1* levels induce elevated putrescine levels, promoting the generation of *TYR* (tyrosinase) and facilitating melanin synthesis in human skin (Sridharan et al., 2020). Other candidate genes had multiple functions. *TSPAN8, LRFN2, PLD5, ATP6V1C2, ITGB1BP1, CCDC149, MAML3, LY75*, and *ARHGAP15* correlate with disease (Pan et al., 2015; Onishi et al., 2018; Takagi et al., 2018; Jobst-Schwan et al., 2020; Shah et al., 2020; Verma et al., 2020; Liu et al., 2021; Kessler et al., 2022; Lee et al., 2022; Li et al., 2022; Zhou et al., 2022; Ahmad et al., 2023). *SLC4A7* is related to purine and pyrimidine nucleotide biosynthetic processes (Ali et al., 2022). *TMEM63B* is associated with ion channel activity (Marques et al., 2019; Du et al., 2020). *RBPJ* is related to angiogenesis (Jiang et al., 2022) and somitogenesis (Shi and Stanley, 2003; Ferjentsik et al., 2009). *LRP4* is associated with the development of the nervous system (Shen et al., 2015; DePew and Mosca, 2021). *AKT1* is associated with carbohydrate and glucose metabolism (Toda et al., 2020; Wu et al., 2023). *PEX5L* is related to adipogenesis (Guo et al., 2021). *FNTA* correlates with protein farnesyltransferase activity (Wang et al., 1996). Among the overlapping genes identified through the selection signal scan analysis, *AKT1, ATP6V1C2, GMDS, LRP4, MAML3, PDIA6, PLD5, TMEM63B*, and *TSPAN8* were detected through GWAS. Notably, *GMDS* and *PDIA6* are markedly associated with pigment deposition in both analysis. Haplotype analysis indicates that the 2 genes allow for a significant differentiation between Brown Tsaiya ducks and those with other plumage colors. Furthermore, there were significant differences in the genotype frequencies for *GMDS* and *PDIA6*; however, the SNPs were in the intronic regions. Given the roles of these genes in pigment deposition, it was hypothesized that the genetic basis of the red plumage phenotype is complex, possibly involving multiple genes.

In the Brown Tsaiya and Ji'an Red ducks, distinct significant peaks were not detected in the red/white group of the association analysis. This could be attributed to the influence of interactions among genes or the hierarchical dominance order of feather colors in ducks, with white feathers exhibiting precedence over red feathers. Hence, gene effects may not be detectable at the genomic level.

In this study, we performed selection signal scans (using methods such as Fst, $\theta\pi$ ratio, and XP-CLR) to identify selection signatures. We simultaneously conducted an association mapping analysis to investigate

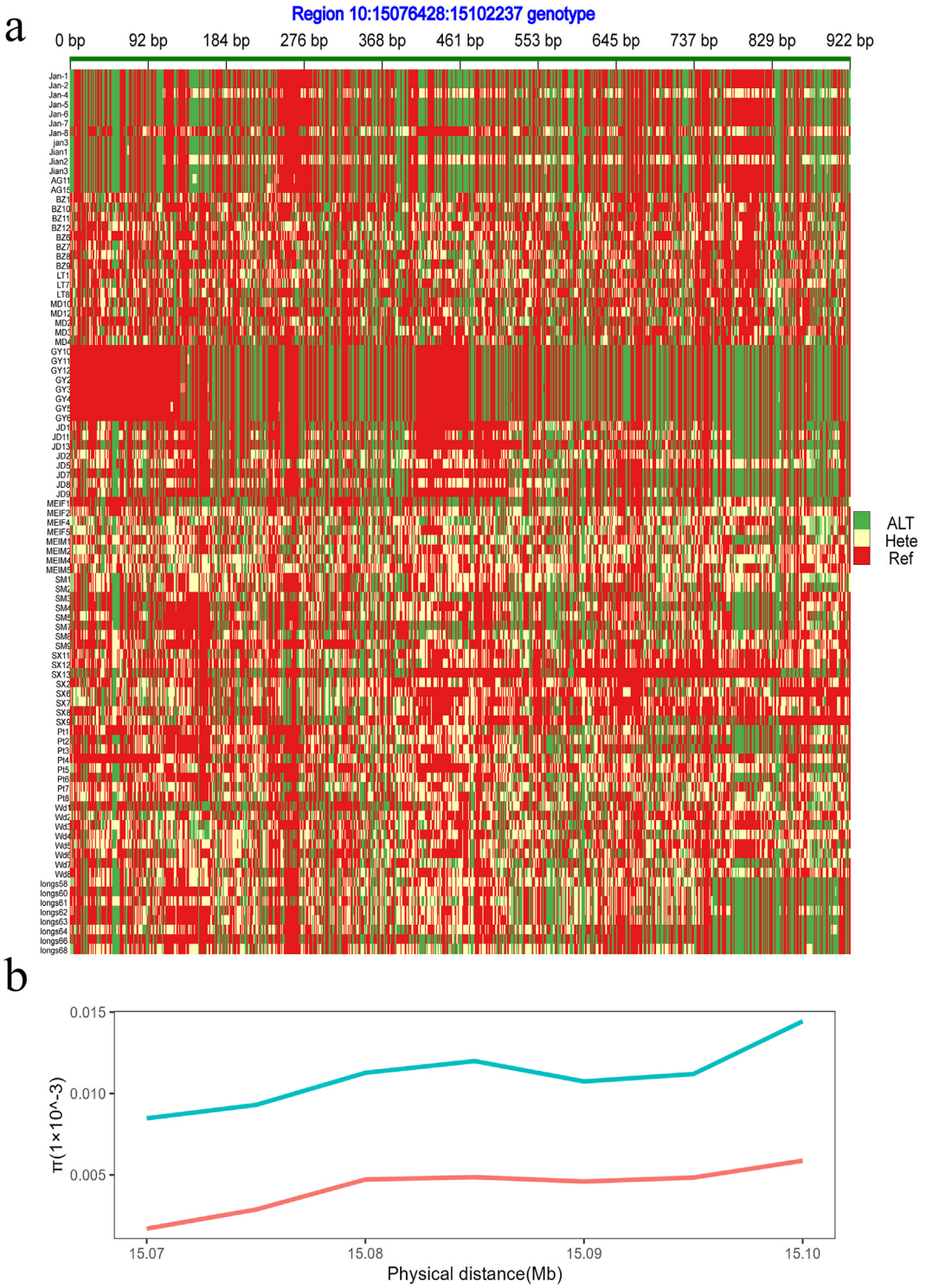

Figure 4. Haplotype and nucleotide diversities in *ENSAPLG00000012679* regions. (A) Heatmap in *ENSAPLG00000012679* regions. (B) Nucleotide diversity in *ENSAPLG00000012679* regions. Red represents Ji'an Red duck; blue represents ducks with other plumage color.

the genetic basis of the red plumage phenotype. GWAS was designed based on a case-control approach, comparing red plumage color ducks to different plumage color ducks. This design facilitated the precise localization of candidate genes influencing plumage color through overlap between multiple methods.

However, there were some limitations that could introduce ambiguity in interpreting the selected signals. The overlapping genes identified in our analysis may be associated with the distinction between red plumage and other phenotypes and with signals of breed-specific selection that occurred during the domestication process, potentially related to other traits. Further studies are required to validate these candidate genes.

The study revealed potential candidate genes involved in the formation of the red plumage phenotype in duck populations. Specifically, *ENSAPLG00000012679, ENPP1, ULK1, GMDS, PDIA6*, and *ODC1* were the

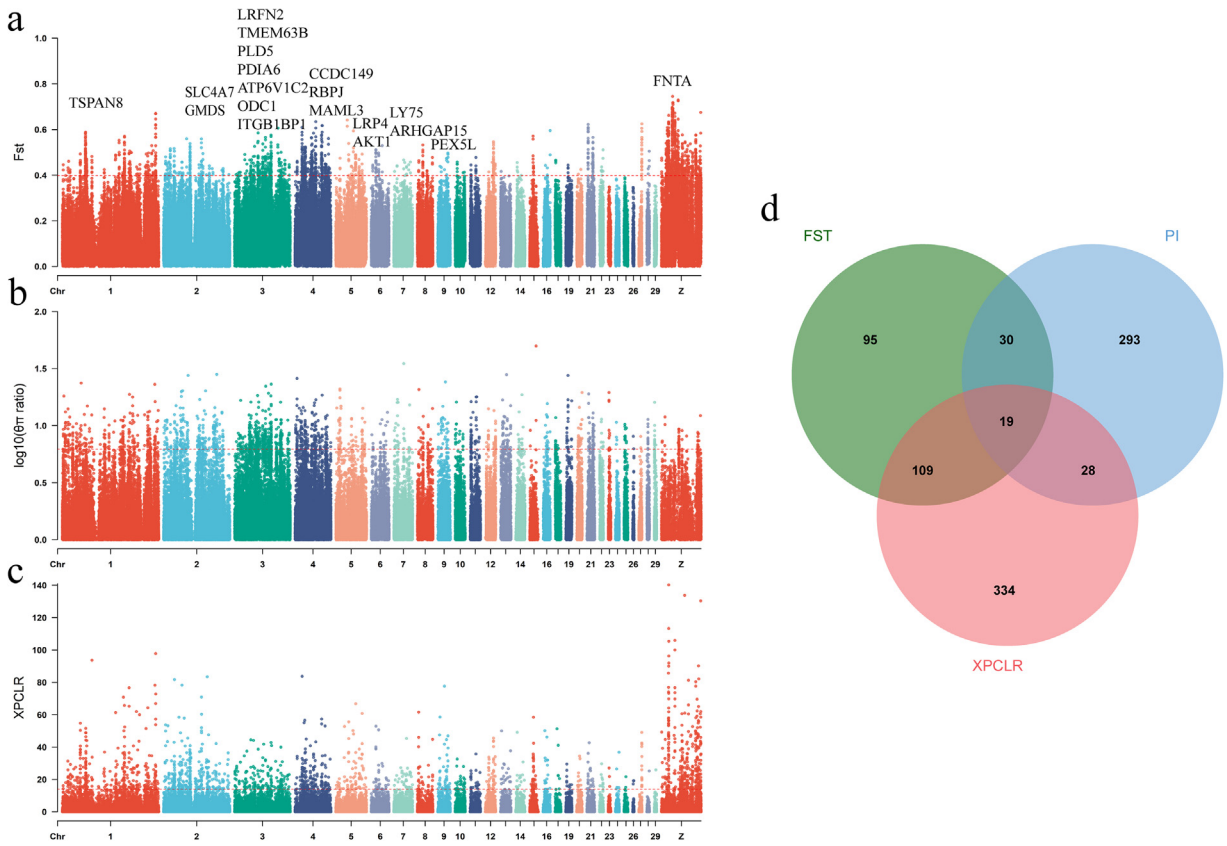

Figure 5. Selective signals of red plumage color in Brown Tsaiya ducks. (A) Genome wide distribution of Fst. (B) Genome wide distribution of $\theta\pi$ ratio. (C) Genome wide distribution of XP-CLR. d. Fst, $\theta\pi$ ratio, and XP-CLR screened for overlapping genes.

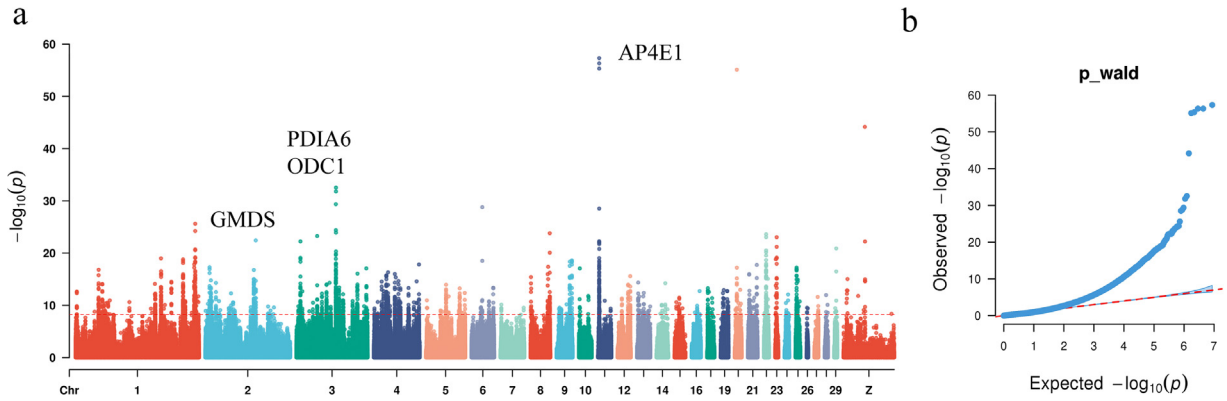

Figure 6. Genome-wide association study for red plumage in Brown Tsaiya ducks. (A) Manhattan plot of genome-wide association study. (B) Quantile−quantile (Q−Q) plots from the genome-wide association analysis (**GWAS**).

Table 3. Overlapping significant regions identified through Fst, pi, and cross-population composite likelihood ratio (**XP-CLR**) and associated genes in Brown Tsaiya ducks.

Gene	Full name	Chromosome	Location (bp)[1]	Length (bp)[1]	Number (SNP)[2]
TSPAN8	Tetraspanin 8	1	37426355-37505746	79391	2
SLC4A7	Solute carrier Family 4 Member 7	2	40756860-41023690	266830	0
GMDS	GDP-mannose 4,6-dehydratase	2	79265182-79671011	405829	67
LRFN2	Leucine-rich repeat and fibronectin type III domain containing 2	3	31578187-31799373	221186	0
TMEM63B	Transmembrane protein 63B	3	33884914-33910150	25236	9
PLD5	Phospholipase D family member 5	3	39264361-39411447	147086	1
PDIA6	Protein disulfide isomerase family A member 6	3	76340827-76361379	20552	1
ATP6V1C2	ATPase H+ transporting V1 subunit C2	3	76352052-76370640	18588	1
ODC1	Ornithine decarboxylase 1	3	76457110-76500422	43312	0
ITGB1BP1	Integrin subunit beta 1 binding protein 1	3	77064448-77071033	6585	1
CCDC149	Coiled-coil domain containing 149	4	35632538-35680171	47633	0
RBPJ	Recombination signal binding protein for immunoglobulin kappa J region	4	35946940-36092637	145697	0

(*continued*)

Table 3 (*Continued*)

Gene	Full name	Chromosome	Location (bp)[1]	Length (bp)[1]	Number (SNP)[2]
MAML3	Mastermind like transcriptional coactivator 3	4	56585225-56781405	196180	10
LRP4	LDL receptor-related protein 4	5	32874741-32912588	37847	27
AKT1	AKT serine/threonine kinase 1	5	55272740-55337060	64320	16
LY75	Lymphocyte antigen 75	7	20553853-20598781	44928	0
ARHGAP15	Rho GTPase activating protein 15	7	31076813-31407565	330752	0
PEX5L	Peroxisomal biogenesis factor 5 like	9	18643390-18680809	37419	0
FNTA	Farnesyltransferase, CAAX box, alpha	Z	52676230-52686816	10586	0

[1]Source: Reference cau_duck1.0 primary assembly (Ensembl).
[2]The number of genomes significant SNP located in gene identified in genome-wide association analysis.

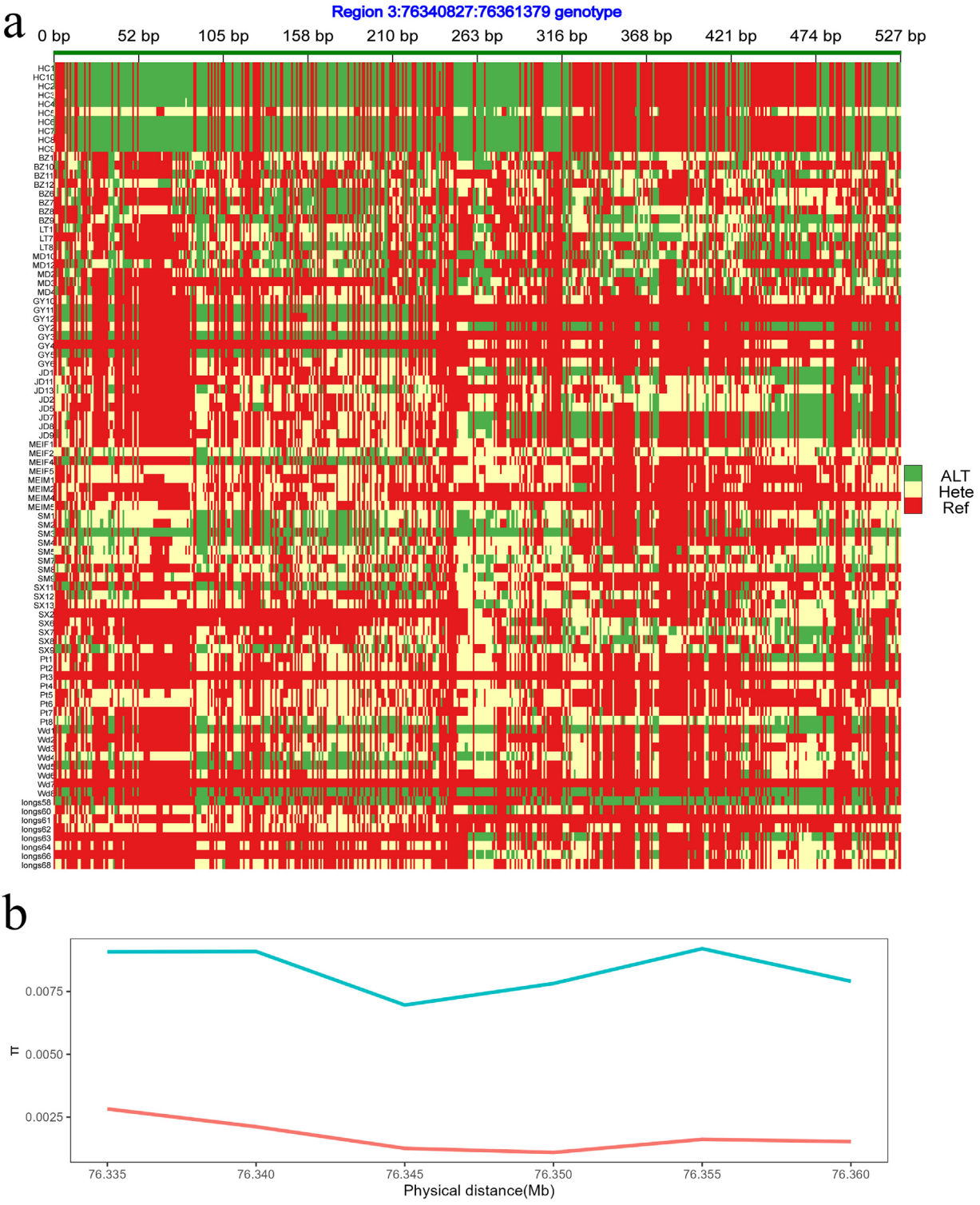

Figure 7. Haplotype and nucleotide diversities in *PDIA6* regions. (A) Heatmap in *PDIA6* regions. (B) Nucleotide diversity in *PDIA6* regions. Red represents the Brown Tsaiya duck; blue represents ducks with other plumage color.

candidate genes associated with the formation of the red plumage phenotype in ducks. This study contributes to a deeper understanding of the duck plumage color genetics, highlighting the complexity of the trait's formation and providing new insights into the variation and selection of the red plumage phenotype in Ji'an Red ducks and Brown Tsaiya ducks, which is essential for breeding purposes.

ACKNOWLEDGMENTS

This work was supported by the Beijing Agriculture Innovation Consortium [grant numbers BAIC06-2023] and supported by the High-performance Computing Platform of China Agricultural University.

DISCLOSURES

The authors declare no conflicts of interest.

SUPPLEMENTARY MATERIALS

Supplementary material associated with this article can be found in the online version at doi:10.1016/j.psj.2024.103694.

REFERENCES

Ahmad, S. M. S., H. Nazar, M. M. Rahman, R. S. Rusyniak, and A. Ouhtit. 2023. ITGB1BP1, a novel transcriptional target of CD44-downstream signaling promoting cancer cell invasion. Breast Cancer (Dove Med. Press) 15:373–380.

Ali, E. S., A. Liponska, B. P. O'Hara, D. R. Amici, M. D. Torno, P. Gao, J. M. Asara, M. F. Yap, M. L. Mendillo, and I. Ben-Sahra. 2022. The mTORC1-SLC4A7 axis stimulates bicarbonate import to enhance de novo nucleotide synthesis. Mol. Cell. 82:3284–3298.

Berry, R., L. Harewood, L. Pei, M. Fisher, D. Brownstein, A. Ross, W. A. Alaynick, J. Moss, N. D. Hastie, P. Hohenstein, J. A. Davies, R. M. Evans, and D. R. FitzPatrick. 2011. Esrrg functions in early branch generation of the ureteric bud and is essential for normal development of the renal papilla. Hum. Mol. Genet. 20:917–926.

Browning, B. L., Y. Zhou, and S. R. Browning. 2018. A one-penny imputed genome from next-generation reference panels. Am. J. Hum. Genet. 103:338–348.

Buchert, R., A. I. Nesbitt, H. Tawamie, I. D. Krantz, L. Medne, I. Helbig, D. R. Matalon, A. Reis, A. Santani, H. Sticht, and R. Abou Jamra. 2016. SPATA5 mutations cause a distinct autosomal recessive phenotype of intellectual disability, hypotonia and hearing loss. Orphanet J. Rare Dis. 11:130.

Chang, C. C., C. C. Chow, L. C. A. M. Tellier, S. Vattikuti, S. M. Purcell, and J. J. Lee. 2015. Second-generation PLINK: rising to the challenge of larger and richer datasets. Gigascience 4:7.

Chen, S. F., Y. Q. Zhou, Y. R. Chen, and J. Gu. 2018. fastp: an ultra-fast all-in-one FASTQ preprocessor. Bioinformatics 34:884–890.

Chourabi, M., M. S. Liew, S. Lim, D. H'Mida-Ben Brahim, L. Boussofara, L. Dai, P. M. Wong, J. N. Foo, B. Sriha, K. S. Robinson, S. Denil, J. E. Common, O. Mamai, Y. Ben Khalifa, M. Bollen, J. Liu, M. Denguezli, C. Bonnard, A. Saad, and B. Reversade. 2018. ENPP1 mutation causes recessive cole disease by altering melanogenesis. J. Invest. Dermatol. 138:291–300.

Danecek, P., A. Auton, G. Abecasis, C. A. Albers, E. Banks, M. A. DePristo, R. E. Handsaker, G. Lunter, G. T. Marth, S. T. Sherry, G. McVean, R. Durbin, and G. P. A. Grp. 2011. The variant call format and VCFtools. Bioinformatics 27:2156–2158.

DePew, A. T., and T. J. Mosca. 2021. Conservation and innovation: versatile roles for LRP4 in nervous system development. J. Dev. Biol. 9:9.

Du, H., C. Ye, D. Wu, Y. Y. Zang, L. Zhang, C. Chen, X. Y. He, J. J. Yang, P. Hu, Z. Xu, G. Wan, and Y. S. Shi. 2020. The cation channel TMEM63B is an osmosensor required for hearing. Cell Rep 31:107596.

Eytan, O., F. Morice-Picard, O. Sarig, K. Ezzedine, O. Isakov, Q. Li, A. Ishida-Yamamoto, N. Shomron, T. Goldsmith, D. Fuchs-Telem, N. Adir, J. Uitto, S. J. Orlow, A. Taieb, and E. Sprecher. 2013. Cole disease results from mutations in ENPP1. Am. J. Hum. Genet. 93:752–757.

Ferjentsik, Z., S. Hayashi, J. K. Dale, Y. Bessho, A. Herreman, B. De Strooper, G. Del Monte, J. L. De La Pompa, and M. Maroto. 2009. Notch is a critical component of the mouse somitogenesis oscillator and is essential for the formation of the somites. PLoS Genet 5:e1000662.

Gao, H., B. Sun, H. Fu, X. Chi, F. Wang, X. Qi, J. Hu, and S. J. O. Shao. 2016. PDIA6 promotes the proliferation of HeLa cells through activating the Wnt/β-catenin signaling pathway. Oncotarget 7:53289.

Gunnarsson, U., S. Kerje, B. Bed'hom, A. S. Sahlqvist, O. Ekwall, M. Tixier-Boichard, O. Kämpe, and L. Andersson. 2011. The Dark brown plumage color in chickens is caused by an 8.3-kb deletion upstream of SOX10. Pigment Cell Melanoma Res 24:268–274.

Guo, L., X. Chao, W. Huang, Z. Li, K. Luan, M. Ye, S. Zhang, M. Liu, H. Li, W. Luo, Q. Nie, X. Zhang, and Q. Luo. 2021. Whole transcriptome analysis reveals a potential regulatory mechanism of LncRNA-FNIP2/miR-24-3p/FNIP2 axis in chicken adipogenesis. Front. Cell Dev. Biol. 9:653798.

Hider, J. L., R. M. Gittelman, T. Shah, M. Edwards, A. Rosenbloom, J. M. Akey, and E. J. Parra. 2013. Exploring signatures of positive selection in pigmentation candidate genes in populations of East Asian ancestry. BMC Evol. Biol. 13:150.

Ho, H., R. Kapadia, S. Al-Tahan, S. Ahmad, and A. K. Ganesan. 2011. WIPI1 coordinates melanogenic gene transcription and melanosome formation via TORC1 inhibition. J. Biol. Chem. 286:12509–12523.

Hua, G., J. Chen, J. Wang, J. Li, and X. Deng. 2021. Genetic basis of chicken plumage color in artificial population of complex epistasis. Anim. Genet. 52:656–666.

Huang, T., Y. Pu, C. Song, Z. Sheng, and X. Hu. 2020. A quantitative trait locus on chromosome 2 was identified that accounts for a substantial proportion of phenotypic variance of the yellow plumage color in chicken. Poult. Sci. 99:2902–2910.

Jiang, F., R. Lin, C. Y. Xiao, T. H. Xie, Y. X. Jiang, J. H. Chen, P. Ni, W. K. Sung, J. L. Han, X. Y. Du, and S. J. Li. 2021. Analysis of whole-genome re-sequencing data of ducks reveals a diverse demographic history and extensive gene flow between Southeast/South Asian and Chinese populations. Genet. Sel. Evol. 53:35.

Jiang, Q., Y. Ma, Y. Zhao, M. D. Yao, Y. Zhu, Q. Y. Zhang, and B. Yan. 2022. tRNA-derived fragment tRF-1001: A novel anti-angiogenic factor in pathological ocular angiogenesis. Mol. Ther. Nucleic Acids. 30:407–420.

Jobst-Schwan, T., V. Klämbt, M. Tarsio, J. F. Heneghan, A. J. Majmundar, S. Shril, F. Buerger, I. Ottlewski, B. E. Shmukler, and R. Topaloglu. 2020. Whole exome sequencing identified ATP6V1C2 as a novel candidate gene for recessive distal renal tubular acidosis. Kidney Int 97:567–579.

Kalie, E., M. Razi, and S. A. Tooze. 2013. ULK1 regulates melanin levels in MNT-1 cells independently of mTORC1. Plos One 8: e75313.

Kerje, S., J. Lind, K. Schutz, P. Jensen, and L. Andersson. 2003. Melanocortin 1-receptor (MC1R) mutations are associated with plumage colour in chicken. Anim. Genet. 34:241–248.

Kessler, M. D., A. Damask, S. O'Keeffe, N. Banerjee, D. Li, K. Watanabe, A. Marketta, M. Van Meter, S. Semrau, J. Horowitz, J. Tang, J. A. Kosmicki, V. M. Rajagopal, Y. Zou, Y. Houvras, A. Ghosh, C. Gillies, J. Mbatchou, R. R. White, N. Verweij, J. Bovijn, N. N. Parikshak, M. G. LeBlanc, M. Jones, C. Regeneron Genetics, G.-R. D. Collaboration, D. J. Glass, L. A. Lotta, M. N. Cantor, G. S. Atwal, A. E. Locke, M. A. R. Ferreira, R. Deering, C. Paulding, A. R. Shuldiner, G. Thurston, A. A. Ferrando, W. Salerno, J. G. Reid, J. D. Overton, J. Marchini, H. M. Kang, A. Baras, G. R. Abecasis,

and E. Jorgenson. 2022. Common and rare variant associations with clonal haematopoiesis phenotypes. Nature 612:301–309.
Kijas, J. M., R. Wales, A. Tornsten, P. Chardon, M. Moller, and L. Andersson. 1998. Melanocortin receptor 1 (MC1R) mutations and coat color in pigs. Genetics 150:1177–1185.
Kinoshita, K., T. Akiyama, M. Mizutani, A. Shinomiya, A. Ishikawa, H. H. Younis, M. Tsudzuki, T. Namikawa, and Y. Matsuda. 2014. Endothelin receptor B2 (EDNRB2) is responsible for the tyrosinase-independent recessive white (mow) and mottled (mo) plumage phenotypes in the chicken. PLoS One 9:e86361.
Lee, H., V. Krishnan, L. J. Wirth, C. Nucera, M. Venturina, P. M. Sadow, A. Mita, and W. Sacks. 2022. Case report of CCDC149-ALK fusion: a novel genetic alteration and a clinically relevant target in metastatic papillary thyroid carcinoma. Thyroid. 32:1580–1585.
Li, G., J. Huang, S. Chen, Y. He, Z. Wang, and J. Peng. 2022. High expression of ATP6V1C2 predicts unfavorable overall survival in patients with colon adenocarcinoma. Front. Genet. 13:930876.
Li, H., and R. Durbin. 2009. Fast and accurate short read alignment with Burrows-Wheeler transform. Bioinformatics 25:1754–1760.
Liu, J., J. Li, Y. Ma, C. Xu, Y. Wang, and Y. He. 2021. MicroRNA miR-145-5p inhibits Phospholipase D 5 (PLD5) to downregulate cell proliferation and metastasis to mitigate prostate cancer. Bioengineered 12:3240–3251.
Liu, W., Q. Chen, and Y. Xia. 2023. New mechanistic insights of melasma. Clin. Cosmet. Investig. Dermatol. 16:429–442.
Marques, M. C., I. S. Albuquerque, S. H. Vaz, and G. J. Bernardes. 2019. Overexpression of osmosensitive Ca2+-permeable channel TMEM63B promotes migration in HEK293T cells. Biochemistry. 58:2861–2866.
McKenna, A., M. Hanna, E. Banks, A. Sivachenko, K. Cibulskis, A. Kernytsky, K. Garimella, D. Altshuler, S. Gabriel, M. Daly, and M. A. DePristo. 2010. The genome analysis toolkit: a MapReduce framework for analyzing next-generation DNA sequencing data. Genome Res 20:1297–1303.
Nie, C., Z. Zhang, J. Zheng, H. Sun, Z. Ning, G. Xu, N. Yang, and L. Qu. 2016. Genome-wide association study revealed genomic regions related to white/red earlobe color trait in the Rhode Island Red chickens. BMC Genet 17:115.
Onishi, H., S. Ichimiya, K. Yanai, M. Umebayashi, K. Nakamura, A. Yamasaki, A. Imaizumi, S. Nagai, M. Murahashi, H. Ogata, and T. Morisaki. 2018. RBPJ and MAML3: potential therapeutic targets for small cell lung cancer. Anticancer Res 38:4543–4547.
Pan, S. J., Y. B. Wu, S. Cai, Y. X. Pan, W. Liu, L. G. Bian, B. Sun, and Q. F. Sun. 2015. Over-expression of tetraspanin 8 in malignant glioma regulates tumor cell progression. Biochem. Biophys. Res. Commun. 458:476–482.
Robbins, L. S., J. H. Nadeau, K. R. Johnson, M. A. Kelly, L. Roselli-Rehfuss, E. Baack, K. G. Mountjoy, and R. D. Cone. 1993. Pigmentation phenotypes of variant extension locus alleles result from point mutations that alter MSH receptor function. Cell 72:827–834.
Serra, J. A. 1946. Constitution of hair melanins. Nature 157:771.
Shah, R., V. Sharma, H. Singh, I. Sharma, G. A. Bhat, I. A. Shah, B. Iqbal, R. Rafiq, N. Nissa, M. Muzaffar, M. T. Rasool, G. N. Lone, S. Kaul, M. M. Lone, E. Rai, N. A. Dar, and S. Sharma. 2020. LRFN2 gene variant rs2494938 provides susceptibility to esophageal cancer in the population of Jammu and Kashmir. J. Cancer Res. Ther. 16:S156–S159.
Shen, C., W. C. Xiong, and L. Mei. 2015. LRP4 in neuromuscular junction and bone development and diseases. Bone 80:101–108.
Shi, S., and P. Stanley. 2003. Protein O-fucosyltransferase 1 is an essential component of Notch signaling pathways. Proc. Natl. Acad. Sci. U. S. A. 100:5234–5239.
Sridharan, A., M. Shi, V. I. Leo, N. Subramaniam, T. C. Lim, T. Uemura, K. Igarashi, S. T. Tien Guan, N. S. Tan, and L. A. Vardy. 2020. The polyamine putrescine promotes human epidermal melanogenesis. J. Invest. Dermatol. 140:2032–2040.
Takagi, K., Y. Miki, Y. Onodera, T. Ishida, M. Watanabe, H. Sasano, and T. Suzuki. 2018. ARHGAP15 in human breast carcinoma: a potent tumor suppressor regulated by androgens. Int. J. Mol. Sci. 19:804.
Tanaka, A. J., M. T. Cho, F. Millan, J. Juusola, K. Retterer, C. Joshi, D. Niyazov, A. Garnica, E. Gratz, M. Deardorff, A. Wilkins, X. Ortiz-Gonzalez, K. Mathews, K. Panzer, E. Brilstra, K. L. van Gassen, C. M. Volker-Touw, E. van Binsbergen, N. Sobreira, A. Hamosh, D. McKnight, K. G. Monaghan, and W. K. Chung. 2015. Mutations in SPATA5 are associated with microcephaly, intellectual disability, seizures, and hearing loss. Am. J. Hum. Genet. 97:457–464.
Toda, G., K. Soeda, Y. Okazaki, N. Kobayashi, Y. Masuda, N. Arakawa, H. Suwanai, Y. Masamoto, Y. Izumida, N. Kamei, T. Sasako, R. Suzuki, T. Kubota, N. Kubota, M. Kurokawa, K. Tobe, T. Noda, K. Honda, D. Accili, T. Yamauchi, T. Kadowaki, and K. Ueki. 2020. Insulin-and lipopolysaccharide-mediated signaling in adipose tissue macrophages regulates postprandial glycemia through Akt-mTOR activation. Mol. Cell. 79:43–53.
Vage, D. I., H. Klungland, D. Lu, and R. D. Cone. 1999. Molecular and pharmacological characterization of dominant black coat color in sheep. Mamm. Genome. 10:39–43.
Verma, S., D. Bakshi, V. Sharma, I. Sharma, R. Shah, A. Bhat, G. R. Bhat, B. Sharma, A. Wakhloo, S. Kaul, V. Heer, A. Bhat, D. Abrol, V. Verma, and R. Kumar. 2020. Genetic variants of DNAH 11 and LRFN 2 genes and their association with ovarian and breast cancer. Int. J. Gynecol. Obstet. 148:118–122.
Wang, T., P. D. Danielson, B. Y. Li, P. C. Shah, S. D. Kim, and P. K. Donahoe. 1996. The p21(RAS) farnesyltransferase alpha subunit in TGF-beta and activin signaling. Science 271:1120–1122.
Wang, R., J. L. Sun, H. Han, Y. F. Huang, T. Chen, M. M. Yang, Q. Wei, H. F. Wan, and Y. Y Liao. 2021. Whole-genome resequencing reveals genetic characteristics of different duck breeds from the Guangxi region in China. G3 (Bethesda) 11:jkab054.
Wu, L. X., Y. C. Xu, K. Pantopoulos, X. Y. Tan, X. L. Wei, H. Zheng, and Z. Luo. 2023. Glycophagy mediated glucose-induced changes of hepatic glycogen metabolism via OGT1-AKT1-FOXO1(Ser238) pathway. J. Nutr. Biochem. 117:109337.
Yang, L., X. Du, S. Wei, L. Gu, N. Li, Y. Gong, and S. Li. 2017. Genome-wide association analysis identifies potential regulatory genes for eumelanin pigmentation in chicken plumage. Anim. Genet. 48:611–614.
Yu, W., C. Wang, Q. Xin, S. Li, Y. Feng, X. Peng, and Y. Gong. 2013. Non-synonymous SNPs in MC1R gene are associated with the extended black variant in domestic ducks (Anas platyrhynchos). Anim. Genet. 44:214–216.
Zhang, W., M. Jin, Z. Lu, T. Li, H. Wang, Z. Yuan, and C. Wei. 2023a. Whole genome resequencing reveals selection signals related to wool color in sheep. Animals (Basel). 13:3265.
Zhang, X. Y., T. Zhu, L. Wang, X. Z. Lv, W. F. Yang, C. Q. Qu, H. Y. Li, H. E. Wang, Z. H. Ning, and L. J. Qu. 2023b. Genome-wide association study reveals the genetic basis of duck plumage colors. Genes (Basel) 14:856.
Zhang, Z., Y. Jia, P. Almeida, J. E. Mank, M. van Tuinen, Q. Wang, Z. Jiang, Y. Chen, K. Zhan, S. Hou, Z. Zhou, H. Li, F. Yang, Y. He, Z. Ning, N. Yang, and L. Qu. 2018. Whole-genome resequencing reveals signatures of selection and timing of duck domestication. Gigascience 7:giy027.
Zhou, X., and M. Stephens. 2012. Genome-wide efficient mixed-model analysis for association studies. Nat. Genet. 44:821–U136.
Zhou, Y., L. Xu, J. Wang, B. Ge, Q. Wang, T. Wang, C. Liu, B. Wei, Q. Wang, and Y. Gao. 2022. LRFN2 binding to NMDAR inhibits the progress of ESCC via regulating the Wnt/β-Catenin and NF-κB signaling pathway. Cancer Sci 113:3566–3578.
Zhou, Z. K., M. Li, H. Cheng, W. L. Fan, Z. R. Yuan, Q. Gao, Y. X. Xu, Z. B. Guo, Y. S. Zhang, J. Hu, H. H. Liu, D. P. Liu, W. H. Chen, Z. Q. Zheng, Y. Jiang, Z. G. Wen, Y. M. Liu, H. Chen, M. Xie, Q. Zhang, W. Huang, W. Wang, S. S. Hou, and Y. Jiang. 2018. An intercross population study reveals genes associated with body size and plumage color in ducks. Nat. Commun. 9:2648.
Zhu, T., X. Qi, Y. Chen, L. Wang, X. Z. Lv, W. F. Yang, J. W. Zhang, K. Y. Li, Z. H. Ning, Z. H. Jiang, and L. J. Qu. 2021. Positive selection of skeleton-related genes during duck domestication revealed by whole genome sequencing. BMC Ecol. Evol. 21:165.